A Time-Domain Technique for Computation of Noise Spectral Density in Linear and Non-linear Time-Varying Circuits

V.Vasudevan

Department of Electrical Engineering

Indian Institute of Technology

Madras 600036

vinita@ee.iitm.ernet.in

Abstract

This paper presents a new time domain technique for computing the noise spectral density. The power spectral density is interpreted as the asymptotic value of the expected energy spectral density per unit time. We show that the methodology of stochastic differential equations can be used to derive a set of ordinary differential equations for the expected energy spectral density. This set of equations can then be integrated in time until the steady state value of the power spectral density is obtained. The method is quite general and can be used to find the noise spectrum in any circuit in which noise can be treated as a perturbation. Both the noise variance and the power spectral density are obtained. The general nature of this algorithm has been illustrated in this paper by using it to get the noise spectral density in switched capacitor circuits, externally linear circuits and oscillators. The results match well with published experimental/analytical data.
Keywords: noise, power spectral density, analog circuits

I. INTRODUCTION

With decreasing power supply voltages and tight dynamic range specifications, we require simple and accurate methods for computation of the output noise variance and power spectral density (PSD).While the adjoint method proposed by Rohrer [1] has been used successfully for linear time-invariant circuits, several methods have been proposed for time-varying linear and non-linear circuits. These methods are typically applicable to a particular circuit or a class of circuits. Broadly they can be classified as methods for linear periodically switched systems, periodically varying circuits with single or multi-tone excitations, externally linear circuits and methods to compute phase noise in oscillators.

Noise in periodically switched linear systems has received considerable attention. Most of these studies pertain to switched capacitor(SC) circuits. One of the early attempts was made by Rice [2]. He computed the noise spectral density at the output of a periodically switched RC circuit, driven by white noise. Strom and Signell [3] obtained closed form solutions for the time-varying impulse response and the transfer function for periodically switched linear circuits. They used this to obtain the output noise spectral density. Fisher [4] computes the noise spectral density by converting the SC circuit to an equivalent RC circuit. The actual computation is done using SPICE and it requires knowledge of the noise bandwidth, which is not readily available. Maloberti *et al* [5] have computed the noise spectrum of a switched capacitor integrator, including opamp non-idealities. Goette *et al* [6], [7] compute the time

averaged autocorrelation matrix by solving the Lyapunov equation. Using the "full and fast" charge transfer assumption, they solve the z-domain equations of the discrete time system to get the noise spectral density. They have an approximate implementation for the "sample and held" portion of the noise alone. Toth *et al* [8] use the charge state variable form of the equations and obtain the noise spectral density based on the time-varying transfer function. They also use the "full and fast" charge transfer approximation and obtain simplified expressions for noise in ideal switched capacitor networks. They consider both thermal as well as $1/f$ noise. The adjoint network approach has been explored in [9], [10], [11], [12]. The method proposed by Yuan *et al* does not require the "full and fast" charge transfer approximation. Dong *et al* [13] obtain the noise in SC circuits, including sigma-delta modulators, by using random-pulse waveforms to model noise sources.

There have also been several attempts at noise analysis for periodically varying nonlinear and externally linear systems. In all these cases, noise is regarded as a small perturbation and the circuit is linearized around the large signal steady state solution. The linear periodic transfer function is then used to get the time-varying autocorrelation and the power spectral density. Okumura *et al* [14] have analyzed noise in periodically switched circuits and nonlinear circuts with periodic large signal excitations. They use a sampled form of the time-varying transfer function. Roychowdhury *et al* [15] have extended the algorithm of Strom and Signell for noise analysis of RF circuits, including cyclostationary noise sources. Using the concept of harmonic PSDs, they propose an efficient harmonic balance based algorithm to compute the noise spectrum. Noise in externally linear systems has also been studied extensively. These circuits have cyclostationary noise sources as well as signal-noise intermodulation. These circuits are nonlinear as far as noise sources are concerned. If noise can be regarded as a perturbation, a linear periodically varying transfer function can be obtained (for a periodic input excitation). Mulder *et al* [16], [17] find the time-varying autocorrelation function. The time-dependent frequency spectrum is obtained as the Fourier transform of the autocorrelation. Toth *et al* [18], [19] obtain the output noise spectral density based on the time-varying noise transfer functions.

In the case of phase noise, several methods have been proposed. A heuristic expression based on the Q of a feedback oscillator was obtained by Leeson [20]. Razavi [21] obtained the spectrum of the ring oscillator using a linear time-invariant transfer function. Kurokawa [25] and

Okumura *et al* [26] obtain the spectrum by computing the linear time-varying transfer function. Noise and timing jitter in ring oscillators were also studied by McNeill [22] and Weigandt *et al* [23] using stationary and time-varying noise sources respectively. Timing jitter in relaxation oscillators was obtained by Abidi *et al* [24]. In all these cases, timing jitter is obtained by finding the standard deviation of the error in the zero crossings of the oscillator. Methods based on a nonlinear analysis include [27], [28], [29]. De Smedt *et al* [27] compute the phase noise by doing a transient simulation, but sinusoidal sources at carefully selected frequencies are used to model noise. Hajimiri *et al* [28] find a linear periodic impulse sensitivity function(ISF) for the oscillator and use it to compute the phase variations due to noise. They regard the oscillator as a phase modulating system to convert the phase to a voltage. The method proposed by Demir *et al* [29] is based on previous work by Lax and Kaertner [30], [31]. They do a nonlinear perturbation analysis to get the Lorentzian noise spectrum about each harmonic and also propose an efficient method to compute it.

Practically all the techniques proposed are frequency domain techniques that are applicable to a particular circuit or a class of circuits. Among the time-domain methods, the Monte-Carlo technique can, of course, be used for all circuits. However, it is computationally very expensive. A method based on stochastic differential equations has been used by Demir *et al* [32] to get the time-varying covariance matrix of nonlinear circuits. It has been used to predict phase noise of oscillators [31], [32], [29], noise in PLLs [33], the covariance matrix in switched capacitor circuits [6] and the non-stationary noise response in readout circuits used with image sensors [34]. It can be used for all circuits that can be described by differential equations and in which noise can be treated as a perturbation. However, although Demir *et al* suggest that the instantaneous spectral density can be obtained after computing the time-varying autocorrelation, there are no published computations of either the instantaneous or average power spectral density using this method.

In this paper, a new time-domain technique to obtain the average and instantaneous power spectral density is proposed. It is based on stochastic differential equations. It uses the results obtained by Demir *et al* for the covariance matrix. Unlike all previous methods, which essentially use the time-varying autocorrelation/transfer function, we compute the power spectral density using its definition as the limiting value of the energy spectral density per unit time. We

show that a set of ordinary differential equations can be derived for the energy spectral density. These equations can easily be incorporated in any standard circuit simulator. Previous techniques to compute the power spectral density are restricted to certain classes of circuits. The proposed method is applicable to all circuits that can be simulated using a standard circuit simulator, even those in which the noise is nonstationary. Complex device models can be used, though simulations will have to be done in a hierarchical manner for numerical efficiency. The assumption made is that noise can be treated as a perturbation. To the best of the author's knowledge, other than Monte-Carlo analysis, this is the only time-domain technique to obtain the average noise spectral density.

The paper is organized as follows. Sections II and III contain relevant definitions and a derivation of the equations. Section IV summarizes the steps involved in the computation and the numerical methods used in the implementation of the algorithm. The proposed method is validated by comparing the simulated results with published data for three types of circuits - switched capacitor circuits, externally linear circuits and oscillators. Section V contains the simulation results and a comparison with published data. The advantages and limitations of the method are discussed in the conclusions. For all the simulations performed, only thermal noise sources have been considered and instead of the full device models, simpler macromodels are used.

II. Some Definitions and an Outline of the proposed Technique

The power spectral density can be interpreted as the limiting value of the expected energy spectral density per unit time [35], [36], [37]. This is done as follows. Let $v_T(t)$ represent a finite section of the waveform defined as:

$$\begin{aligned} v_T(t) &= v(t), \qquad |t| \leq T/2 \\ &= 0, \qquad |t| > T/2 \end{aligned}$$

Let $V_T(f)$ represent its Fourier transform. It is then possible to define the expected energy spectral density of this finite segment of the waveform, $(ESD)_T$, as:

$$(ESD)_T = E\{|V_T(f)|^2\}$$

where $E\{.\}$ denotes the expectation operator. It can be proved that the expected power spectral density is given by [35], [36], [37]:

$$PSD = \lim_{T\to\infty} \frac{(ESD)_T}{T} \tag{1}$$

When the noise in the circuit is stationary, the PSD as defined by equation (1) is the Fourier transform of the autocorrelation function [35], [36]. If the noise is non-stationary, it can be shown that [37]:

$$\frac{d(ESD)_T}{dt} = S_v(t, f) \tag{2}$$

Here $S_v(t, f)$ is the instantaneous power spectral density and is the Fourier transform of the time-varying autocorrelation function. Therefore the PSD, as defined by equation (1) is the average value of the instantaneous spectral density.

Based on these definitions, a new method to find the average power spectral density is proposed in this paper. We show that the methodology of stochastic differential equations can be used to obtain a set of ordinary differential equations for the energy spectral density. This can then integrated in time until $(PSD)_T = \frac{(ESD)_T}{T}$ reaches steady state.

III. Details of the method

In the discussion that follows, the state variable form of the equations have been used. This is mainly because it is the most convenient form of equations for externally linear circuits. However, any other form of the circuit equations, modified nodal analysis for example, could equally well be used.

A. Derivation of differential equations for energy and cross-spectral density

The state variable form of the circuit equations without noise sources can be written as:

$$\frac{d\mathbf{x}(t)}{dt} = \mathbf{F}(\mathbf{x}(t), \mathbf{u}(t)) \tag{3}$$

where $\mathbf{x}(t)$ is the vector containing the state variables of the circuit and $\mathbf{u}(t)$ is the vector of large signal excitations to the circuit. This can be solved to get the large signal steady state solution of the circuit, $\mathbf{x}_s(t)$.

With the noise sources added, the solution is assumed to be of the form:

$$\mathbf{x}(t) = \mathbf{x}_s(t) + \mathbf{x}_n(t) \tag{4}$$

where $\mathbf{x}_n(t)$ represents the noise voltages. Since noise is treated as a perturbation, a linearized form of the state equations along with additive noise sources can be used for noise computations. This is not true in the case of externally linear equations, where the translinear principle has to be used to obtain the correct equations. This is discussed in more detail in a later section. The linearized equations can be written as:

$$\frac{d\mathbf{x}_n(t)}{dt} = \mathbf{A}(t)\mathbf{x}_n(t) + \mathbf{B}(t)\mathbf{n}(t) \tag{5}$$

In this set of equations, $\mathbf{A}(t)$ is the Jacobian of $\mathbf{F}(.)$ with respect to x, computed at steady state. $\mathbf{B}(t)$ is a matrix containing the spectral intensity of the noise sources and $\mathbf{n}(t)$ is the vector containing the various noise sources, all of which are assumed to be standard Gaussian white noise processes uncorrelated with each other. The steps involved in the linearization have been discussed in detail in [38].

In a more standard form, equation (5) can be written as:

$$d\mathbf{x}_n(t) = \mathbf{A}(t)\mathbf{x}_n(t)dt + \mathbf{B}(t)d\mathbf{W}(t) \tag{6}$$

where $\mathbf{W}(t)$ represents the Wiener process. Note that this representation is only symbolic. The mathematically meaningful form of this equation is its integral representation [40], [41].

Supposing we wish to find the noise power spectral density at node "N" of the circuit. Let the noise waveform be represented by $x_{nN}(t)$. This noise waveform could be a single state variable or a combination of state variables. For convenience, it is assumed that $x_{nN}(t)$ is a state variable. We define:

$$X(t,\omega) = \int_0^t x_{nN}(\tau)e^{-j\omega\tau}d\tau \tag{7}$$

$X(t,\omega)$ is essentially the Fourier transform of a "t-segment" of the noise waveform. Consider the squared process $Z(t)$ given by:

$$Z(t) = X(t,\omega)X(t,\omega)^*$$

Differentiating with respect to time, we get:

$$\frac{dZ(t)}{dt} = x_{nN}(t)e^{-j\omega t}X(t,\omega)^* + X(t,\omega)x_{nN}^*(t)e^{j\omega t} \tag{8}$$

Taking expectations on both sides, we get the derivative with respect to time of the expected energy spectral density:

$$\frac{d(ESD)_T}{dt} = E\{x_{nN}(t)X(t,\omega)^*\}e^{-j\omega t} + E\{x_{nN}^*(t)X(t,\omega)\}e^{j\omega t} \tag{9}$$

Here $E\{.\}$ denotes the expectation operator. The right hand side of equation (9) gives us the instantaneous power spectral density, $S_v(t,f)$. It is a real quantity as expected. To solve this equation, we require the "cross spectral density" $E\{x_{nN}(t)X(t,\omega)^*\}$. This can be obtained as follows. Consider:

$$\mathbf{y}(t) = \mathbf{x}_n(t)X(t,\omega)^* \tag{10}$$

The differential form of this equation is obtained as:

$$d\mathbf{y}(t) = [d\mathbf{x}_n(t)]X(t,\omega)^* + \mathbf{x}_n(t)x_{nN}^*(t)e^{j\omega t}dt \tag{11}$$

Using (6), this can be written as:

$$d\mathbf{y}(t) = [\mathbf{A}(t)\mathbf{x}_n(t)dt + \mathbf{B}(t)d\mathbf{W}(t)]X(t,\omega)^* + \mathbf{x}_n(t)x_{nN}^*(t)e^{j\omega t}dt \tag{12}$$

Taking expectations and noting that the expectation of the Ito integral is zero [40], [41], we get:

$$\frac{d\mathbf{K}'(t)}{dt} = \mathbf{A}(t)\mathbf{K}'(t) + E\{\mathbf{x}_n(t)x_{nN}^*(t)\}e^{j\omega t} \tag{13}$$

where $\mathbf{K}'(t)$ is the vector of "cross-spectral densities" and the elements of this vector are given by:

$$K_i'(t) = E\{y_i(t)\} = E\left\{x_{ni}(t)X(t,\omega)^*\right\}$$

In order to solve the set of equations (9) and (13), we need the time-varying variance of the state variable "N" of the circuit (for which the PSD is required) and its cross-correlation with all the other state variables of the circuit. These values can be obtained by solving for the time-varying covariance matrix which can be computed as described in [32], [40], [41]. It is re-derived in the following sub-section.

B. Derivation of the time-varying covariance matrix

For convenience, the equation for the covariance matrix is re-derived here using the same notation as in [32].

Using the multi-dimensional Ito formula [40], [41], we get:

$$d(\mathbf{x}_n(t)\mathbf{x}_n(t)^{*T}) = \mathbf{x}_n(t)[d\mathbf{x}_n(t)^*]^T + [d\mathbf{x}_n(t)]\mathbf{x}_n(t)^{*T} + d\mathbf{x}_n(t)d\mathbf{x}_n(t)^{*T} \tag{14}$$

The last term arises due to the non-zero quadratic variation of the Ito integral. Using (6), this can be written as:

$$d(\mathbf{x}_n(t)\mathbf{x}_n(t)^{*T}) = \mathbf{x}_n(t)[\mathbf{x}_n(t)^{*T}\mathbf{A}(t)^{*T}dt + \mathbf{B}(t)^{*T}d\mathbf{W}(t)]+$$

$$[\mathbf{A}(t)\mathbf{x}_n(t)dt + \mathbf{B}(t)d\mathbf{W}(t)]x_n(t)^{*T} + \mathbf{B}(t)\mathbf{B}(t)^T dt \tag{15}$$

Taking expectations on both sides and noting that the expectation of the Ito integral is zero [40], [41], we get:

$$\frac{d\mathbf{K}(t)}{dt} = \mathbf{K}(t)\mathbf{A}(t)^{*T} + \mathbf{A}(t)\mathbf{K}(t) + \mathbf{B}(t)\mathbf{B}(t)^T \tag{16}$$

where

$$K_{ij}(t) = E\{x_{ni}(t)x^*_{nj}(t)\}$$

are elements of the noise covariance matrix. It is a Hermitian matrix.

C. Discussion

Equations (3), (9), (13) and (16) form a complete set of ordinary differential equations which can be solved to get the power spectral density. This basically demonstrates that we can directly use the definition of power spectral density in terms of the energy spectral density for computation of the output noise PSD in a circuit. It gives us a completely different method to solve for both the average and the instantaneous power spectral density. Previously this has always been done using the Wiener-Khintchine theorem, which meant that it was necessary to compute either the time-varying auto-correlation or the transfer function. In the proposed technique, we do not explicitly determine the autocorrelation function. Instead of finding the correlation between time samples of a single waveform to find the PSD, we use its variance and cross-correlation with all the other state variables of the circuit. In the process, all the "cross-spectral densities" are also obtained. This gives us an idea of the relative contributions of various portions of the circuit to the output power spectral density.

One of the advantages of this method is that the same method can be used irrespective of whether the noise is stationary or non-stationary. Also, it is not restricted to any particular class

of circuits and can be used with arbitrary large signal input excitations. The numerical methods required are the same as that used for transient analysis, so the algorithm can very easily be integrated into a standard circuit simulator. In fact, the solution of the covariance matrix has been incorporated in SPICE [32]. The only assumption made is that noise is treated as a perturbation.

D. Alternate derivation of the equations

The same set of equations can also be derived as follows. Equation (7) can be written as:

$$\frac{dX(t,\omega)}{dt} = x_{nN}(t)e^{-j\omega t} \tag{17}$$

An augmented state vector $\mathbf{V}(t)$ can be now be defined as:

$$\mathbf{v}(t) = [x_{n1}(t), x_{n2}(t), ...x_{nN}(t), X(t,\omega)]$$

with the corresponding state matrix:

$$\mathbf{E}(t) = \left[\begin{array}{ccccc|c} & & & & & 0 \\ & & & & & 0 \\ & & A(t) & & & .. \\ & & & & & .. \\ \hline 0 & 0 & .. & .. & e^{-j\omega t} & 0 \end{array}\right]$$

and an excitation matrix:

$$\mathbf{F}(t) = \left[\begin{array}{c} \mathbf{B}(t) \\ 0 \end{array}\right]$$

A set of linear stochastic differential equations is obtained as:

$$d\mathbf{v}(t) = \mathbf{E}(t)\mathbf{v}(t) + \mathbf{F}(t)d\mathbf{W}(t) \tag{18}$$

Using the Ito formula, this set of equations can be converted to a set of ordinary differential equations for the elements of covariance matrix, cross-spectral densities and the energy spectral density.

IV. Steps involved in the Computation

In order to solve for the power spectral density, we have to integrate the set of equations (3), (16), (13) and (9) to get the large signal solution, the time-varying covariance matrix, the cross spectral densities and the energy spectral density. In the general case, for a circuit with arbitrary large signal input excitations and non-stationary noise sources, the computed (and measured) PSD could depend on time and the limit in equation (1) may not converge to a single value (for a particular frequency). To get this (possibly time-dependent) average PSD, the set of equations (3), (16), (13) and (9) have to be integrated simultaneously for each frequency. Since equations (3) and (16) do not depend on the frequency, the computation can be split into two parts. Equations (3) and (16) can be first integrated to get the large signal solution and covariance matrix. This can then used in the set of equations (9) and (13), to get the PSD at different frequencies. This method can be used for all circuits, but for certain classes of circuits, the computation can be made more efficient as indicated below.

In most circuits that are of interest, the limit in equation (1) exists and we have a single value for the average PSD at each frequency. However, the time-varying covariance matrix may or may not go to a steady-state. In the case of periodically varying circuits, if the network is stable, the steady state of the covariance matrix is either constant or periodic in nature. For this case the following steps are used in the computation.

1) Solve the set of non-linear equations (3) to get the periodic large signal steady state solution. This is required in order to compute the time-varying Jacobian matrix $A(t)$ as well as the spectral intensity of the noise sources in the circuit. All methods for noise analysis in time-varying circuits require this step.
2) Solve the set of linear time-varying equations (16) to get the steady state value of the time-varying covariance matrix. This gives the variance at the output node and its cross-correlation with other nodes in the circuit. The covariance matrix is periodic with the same period as either the clock (in circuits such as switched capacitor circuits) or the input signal(eg. translinear circuits).
3) Using the steady state Jacobian and covariance matrix, solve the set of equations (13) and (9) to get the cross-spectral and power spectral densities. This has to be done for each frequency.

It is clear that for periodically varying circuits, only steady state solutions need to be computed. This can be done very efficiently as indicated in [42].

In the case of oscillators, the large signal solution is periodic, but the envelop of the variance increases linearly with time [29]. In this case, the set of equations (3) can be solved seperately to get the large signal steady state solution. This is used to compute the time-varying Jacobian matrix. The set of equations (9), (13) and (16) are then integrated simultaneously to get the PSD.

A. Numerical methods used

A prototype code for this algorithm was written in Python, which is a scripting language. The integrations were done using the trapezoidal rule, which is A-stable and locally third order accurate. Time steps were determined using the estimated local truncation error (obtained using divided differences). For the results shown in this paper, the integration was carried out until change in the PSD over a given period (specified in terms of the number of clock cycles or large signal input period or timesteps) was less than 0.1dB. Some amount of experimentation was required to find this period. It varied from 2-5 clock periods in SC circuits and about 2 periods of the large signal input for externally linear circuits. Convergence behaviour for the oscillator is slightly different and is discussed in the section on phase noise. Zero initial conditions were used. However, the final steady state value of the PSD was found to be independent of the initial conditions. Figure 1 shows the variation of the output PSD at $7.5\ kHz$ as a function of time in a switched capacitor low pass filter.

V. RESULTS

A. Switched capacitor circuits

In this section, the algorithm proposed in this paper has been used to find the PSD of three switched capacitor circuits - a switched RC circuit, a bandpass and a lowpass filter. The circuits are modeled as periodically varying linear circuits. In the simulations performed, simple linear macromodels have been used for operational amplifiers and closed switches are modeled using a constant resistance. Therefore, the noise levels in the circuit are determined by the operating point and do not depend on the signal levels. In many of the switched capacitor circuits, the state equations turn out to be linearly dependent due to the presence of capacitor cutsets. Therefore,

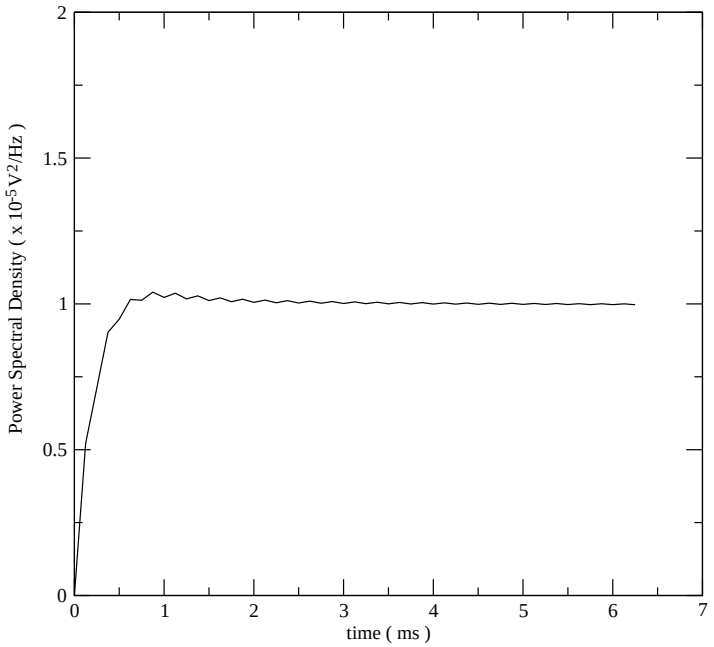

Fig. 1. Power spectral density at $7.5kHz$ as a function of time. This is obtained for a switched capacitor low pass filter. The clock frequency was 4kHz.

the equivalent of the charge state variable form [43] of the equations is used. Charge transfer relationships between capacitors are used to get a complete set of equations for the covariance matrix computation. A typical equation for charge transfer relationship in a switched capacitor circuit can be written as

$$C_1(V_1(t_2) - V_1(t_1)) = C_2(V_2(t_2) - V_2(t_1)) + C_3(V_3(t_2) - V_3(t_1)) + ... \tag{19}$$

This can be easily converted to an equation relating the various cross-correlations K_{ij} between nodes. For example, if

$$C_1\Delta V_1 = C_2\Delta V_2 \tag{20}$$

we get

$$K_{12}(t_2) = K_{12}(t_1) + \frac{C_1}{2C_2}(K_{11}(t_2) - K_{11}(t_1)) + \frac{C_2}{2C_1}(K_{22}(t_2) - K_{22}(t_1)) \tag{21}$$

i.e. since ΔV_2 is completely defined by ΔV_1, the change in the cross-correlation between the two voltages can be obtained from the variance changes alone. As is the case with the differential equations, if there are n charge transfer equations in the switched capacitor circuit, there will be $\frac{(n)(n+1)}{2}$ equations for the time variation of the cross-correlations. These equations replace the corresponding differential equations for the cross-correlations.

1) Periodically switched RC circuit: In order to illustrate the method, details of the equations have been included for the simple case of the periodically switched RC circuit. For this circuit, analytical expressions for the output power spectral density have been obtained by Rice [2]. Figure 2 shows this circuit. The switch is modeled as an ideal switch along with a noisy resistor. The white noise source in this case is the thermal noise current source associated with the switch, i.e. its double-sided PSD is $\frac{2KT}{R}$. The switching time period is T, with a duty cycle of d.

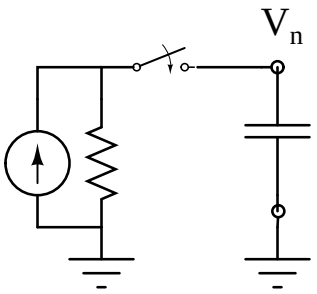

Fig. 2. Periodically switched RC circuit

The stochastic differential equation for this circuit can be written as follows,

$$\begin{aligned} CdV_n(t) &= \frac{-V_n}{R}dt + \sqrt{I}dW(t), \qquad nT \le t \le nT + d\ T \quad (22) \\ &= 0, \qquad nT + d\ T < t \le (n+1)T \quad (23) \end{aligned}$$

In equation (22), I is the magnitude of the power spectral density of the input noise current source, R is the resistance of the switch when closed and W represents the Wiener process. This can be converted to an ordinary differential equation for the variance as described previously. The resulting equation is

$$\begin{aligned} \frac{dK}{dt} &= \frac{-2K}{RC} + \frac{I}{C^2}, \qquad nT \le t \le nT + d\ T \quad (24) \\ \frac{dK}{dt} &= 0, \qquad nT + d\ T < t \le (n+1)T \quad (25) \end{aligned}$$

where $K = E\{V_n V_n^*\}$ is the variance of the noise voltage at the output. This can be easily solved to get the steady state output noise variance. As expected, it is a constant equal to $\frac{KT}{C}$. In order to find the PSD, the state equation is augmented with the following equation:

$$\frac{dV'}{dt} = V_n e^{-j\omega t} \quad (26)$$

Using (9) and (13), the equations for the "cross-spectral density" (K'), and the energy spectral density (K''), can be written as:

In the interval $nT \leq t \leq nT + d\ T$,

$$\frac{dK'}{dt} = -\frac{K'}{RC} + Ke^{j\omega t} \tag{27}$$

$$\frac{dK''}{dt} = 2[Re(K')\cos(\omega t) + Im(K')\sin(\omega t)] \tag{28}$$

For $nT + d\ T < t \leq (n+1)T$

$$\frac{dK'}{dt} = Ke^{j\omega t} \tag{29}$$

$$\frac{dK''}{dt} = 2[Re(K')\cos(\omega t) + Im(K')\sin(\omega t)] \tag{30}$$

The output power spectral density depends on the duty cycle of the clock and the ratio of the clock period to the RC time constant of the circuit. Figure 3 shows a comparison of the simulated results with results obtained using the analytical expressions derived by Rice. It can be seen that they match very well.

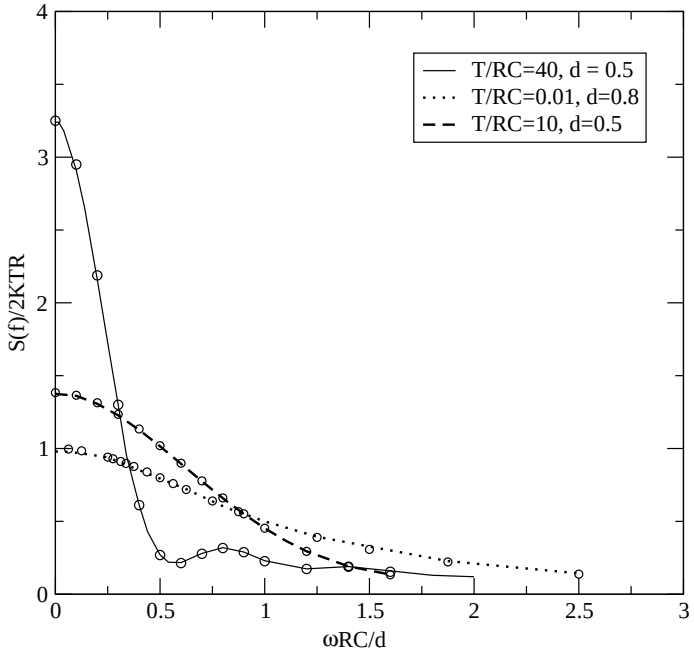

Fig. 3. Comparison of simulated results with the analytical results obtained by Rice[2]. The discrete points are obtained using the analytical expression and the continuous curve represents the simulated results. T is the time period of the clock, d is the duty cycle and RC is the time constant of the circuit. The simulations were done for various combinations of the ratio of the time period to the time constant and the duty cycle.

The sampled data nature of the spectrum arises due to the $\left(\frac{sin(f)}{f}\right)^2$ behaviour that occurs when the noise voltage is held constant. It is seen from the figure that when the noise voltage remains constant for five RC time constants, the spectrum still resembles a continuous time spectrum. It becomes "sampled data like", when the switch remains open for twenty time constants.

2) Switched capacitor bandpass and low pass filter: Figure 4 shows a switched capacitor bandpass filter. The output noise spectral density for this circuit has been obtained by [44] and [12]. The clock frequency is $128kHz$. The switches are modeled using a noisy 80Ω resistor in series with an ideal switch. The input-referred white noise of the operational amplifier was assumed to be $20nV/\sqrt{Hz}$. The opamp was assumed to have infinite unity gain frequency. The above values are as quoted in the literature. The output power spectral density for this filter is shown in Figure 5. It is seen that the results match very well with previously published results.

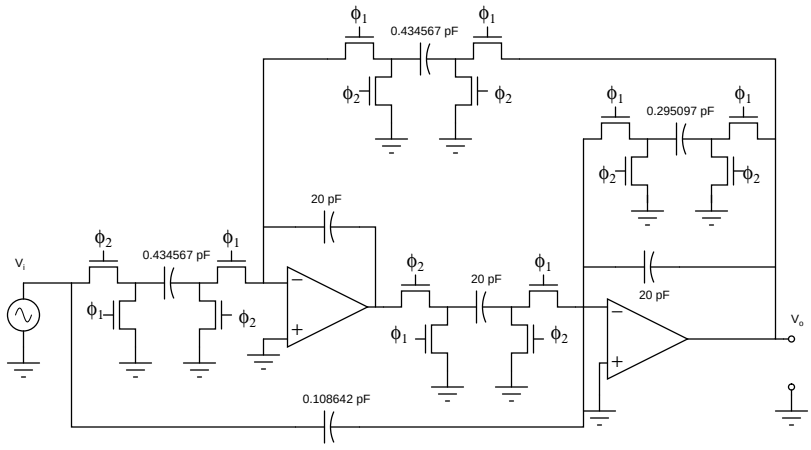

Fig. 4. Switched capacitor bandpass filter[44]

Figure 6 shows a switched capacitor low pass filter. Experimental and theoretical results were published by Toth *et al* [8] for this circuit. The theoretical results obtained however, showed a deep notch at twice the clock frequency which is not seen in the experimental data (since the theoretical results included only the "sample and held" portion of the noise). This circuit was simulated using the algorithm described in this paper. Two different equivalent circuits for the operational amplifier were tried. This is shown in Figure 6. In the first case, the operational amplifier is assumed to have an ideal source follower output. In the second, it is assumed to be a single stage amplifier with a large output resistance (like the folded cascode amplifier), which is often used in switched capacitor circuits. The system of equations (9), (13) and (16)

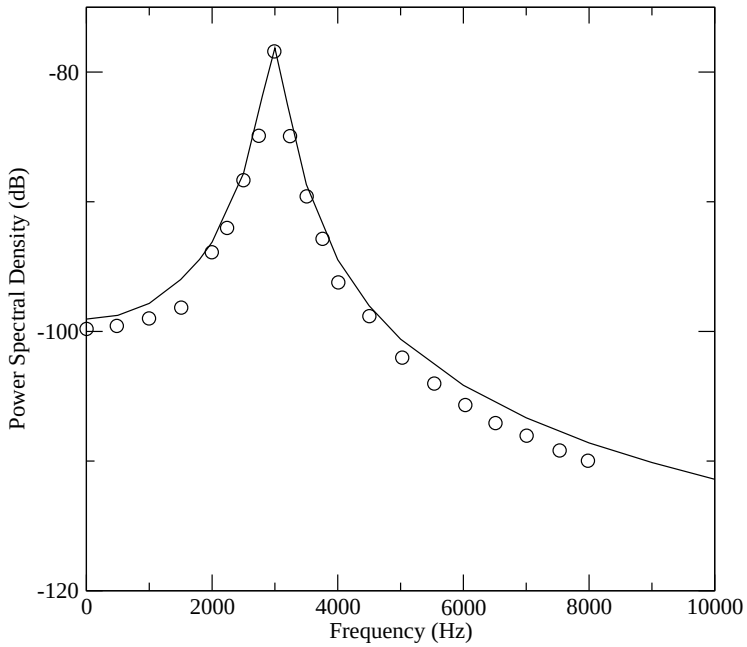

Fig. 5. Output noise spectral density of the bandpass filter. Circles indicate published data[44].

were derived for this circuit. In addition, in the integrating phase, the following charge transfer relationship was used to get all the cross-correlations.

$$C_1\Delta V_1 = C_2\Delta V_2 + C_3\Delta V_3 \tag{31}$$

In order to compare with published data, a white noise source with a PSD of -61.5dB is connected to the non-inverting input of the opamp. The value of the unity gain frequency was taken to be $9\pi \times 10^6$rad/s. Closed switches are modeled using a resistance in parallel with a noise current source. The switch resistance is taken to be 80Ω. The clock frequency is taken to be $4kHz$. The capacitor values were taken to be $300pF$, $100pF$ and $100pF$. These are the values quoted by Toth *et al* [8]. Figure 7 shows a comparison between published experimental data and the simulated results.

When the source follower stage is used, the simulated results match very well with the experimental data with the component values indicated above. In this case, the output noise spectrum depends on the external resistances and capacitances and the unity gain frequency of the opamp alone. The actual value of the capacitance used in the equivalent circuit of the opamp does not matter. If a single stage opamp without a source follower is used, the output additionally depends on the value of the capacitance used in the equivalent circuit of the opamp. For the

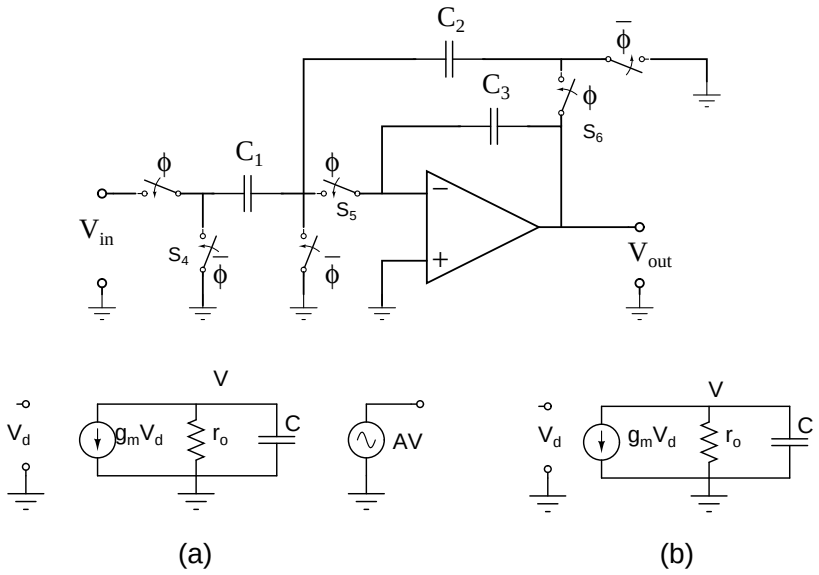

Fig. 6. Low pass filter. (a) and (b) are the two equivalent circuits for the opamp used in the simulations.

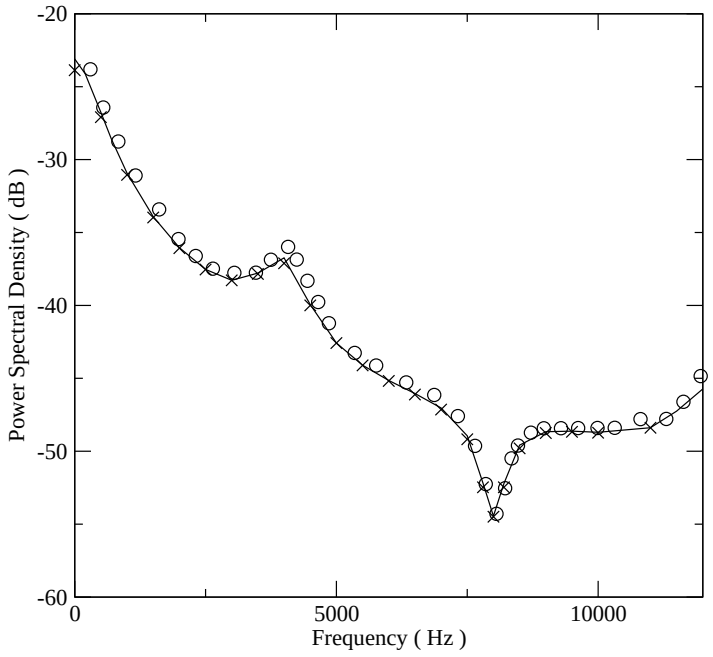

Fig. 7. Comparison between experimental and simulated results. The circles indicate published experimental data[8]. The solid line is the simulated curve obtained when the opamp has a source follower output. The crosses represent simulated data for a single stage opamp with a higher open loop unity gain frequency $(2\pi \times 10^7 rad/s)$ and an equivalent circuit capacitance of $100pF$.

frequency range shown, a good match can be obtained for various combinations of the unity gain frequency and the capacitance value used in the equivalent circuit. For the data plotted in the figure, a unity gain frequency of $2\pi \times 10^7 rad/s$ and a capacitance of $100pF$ was used.

In the case of this low pass filter, the sampled data nature of the spectrum depends very strongly on the noise voltage sampled by C_3. This in turn depends on the resistances of the two switches S_4 and S_5. It is seen from Figure 8, that as the resistances of these two switches increase, the sampled data nature of the output noise spectrum reduces. This is because the transients become slower and the sampled charge on the capacitors reduce. However, as the resistance of S_6 increases, the sampled charge on C_3 increases and spectrum is more strongly "sampled data like". A similar effect occurs with an increase in the unity gain frequency of the

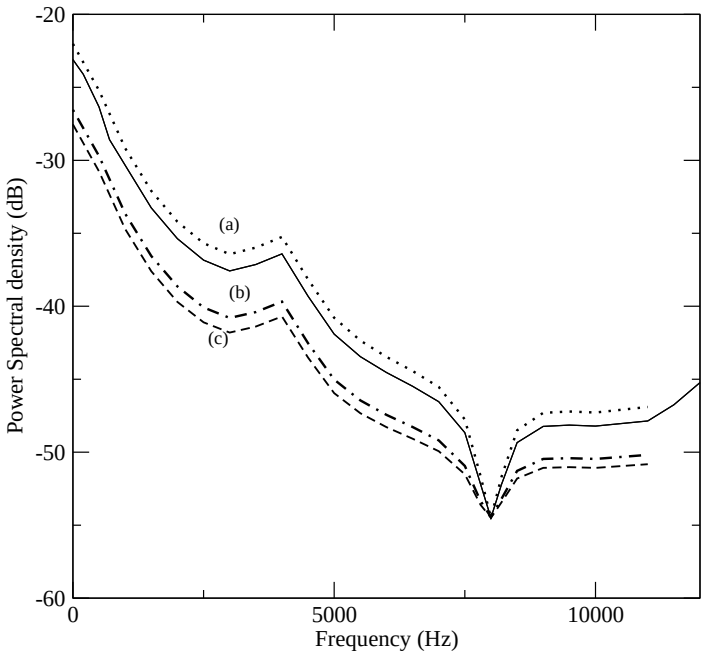

Fig. 8. Output noise spectrum for (a) R6=800Ω, R4=R5=80Ω, (b) R5=800Ω, R4=R6=80Ω and (c) R4=800Ω, R5=R6=80Ω. The solid line is obtained with all three resistor values at 80Ω.

operational amplifier, as seen from Figure 9. As the opamp bandwidth increases, the sampled charge increases resulting in an increase in the spectral density values and also the sampled data nature of the spectrum.

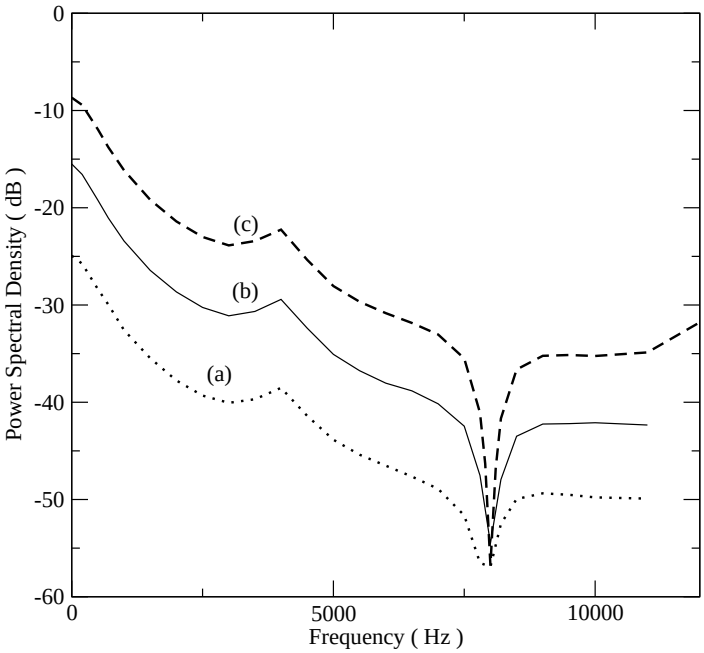

Fig. 9. Output noise spectrum obtained for different values of the opamp unity gain frequency. (a) $\omega_u = 9\pi \times 10^6$rad/s. (b) $\omega_u = 9\pi \times 10^7$rad/s (c) $\omega_u = \infty$.

B. Externally linear circuits

Externally linear circuits are linear as far as the signal is concerned, but are nonlinear for noise. If we regard noise as a small perturbation, it can be modeled as an LTV system for noise analysis and the output SNR can be obtained. Further, if the input excitation is periodic, it is effectively an LPTV system for which the output noise spectral density can be calculated. In this section, results of simulations using the algorithm presented in this paper is compared with experimental and semi-analytical solutions published previously [18], [17]. Experimental results have been obtained for class A and Seevnick's class AB integrator [45] by Toth et al [18]. These two circuits are shown in Figures 10 and 11. In both cases, in order to compare with published experimental data, an external noise generator is connected to the circuit.

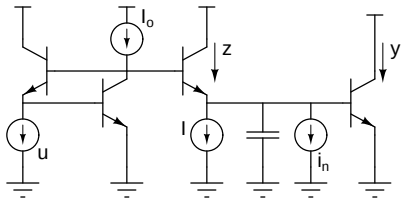

Fig. 10. Class A instantaneously companding circuit

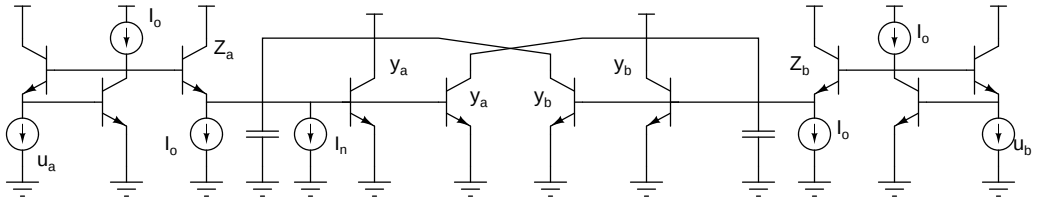

Fig. 11. Class AB instantaneously companding circuit

In the case of externally linear circuits, the translinear principle can be used to get the state equations. In the case of the class A circuit, the state equation can be written as:

$$\frac{dy}{dt} = -ay(t) + ku(t) \tag{32}$$

where

$$a = \frac{I}{CV_T}, \qquad k = \frac{I_o}{CV_T}$$

Equation (32) can be solved to get the large signal steady state solution. Due to the signal-noise intermodulation present in these circuits, it is not possible to use the perturbed state equation with additive noise to get the stochastic differential equation for noise. Once again the translinear principle has to be used. Retaining only first order noise terms, we get:

$$dy_n(t) = -ay_n(t) + \frac{y_s(t)\sqrt{I_n}}{CV_T}dW(t) \tag{33}$$

Here, $y_s(t)$ is the steady state output signal and I_n is the input PSD of the noise source. This can be converted to an equation for the noise variance given by:

$$\frac{dK}{dt} = -\frac{2I}{CV_T}K + \frac{{y_s}^2(t)}{(CV_T)^2}I_n \tag{34}$$

The noise spectral density can then be obtained using this variance. This is shown in Figure 12. It matches well with published experimental data. The values used for the simulation were the same as that quoted by Toth *et al*.

Seevnick's integrator operated in the class B mode was also simulated. As shown in Figure 11, an external noise generator is used. The inputs to the circuit are two "half wave sine" inputs. Once again the stochastic differential equations for noise were obtained using the translinear principle. The equations for the noise variance and cross-correlation are given as:

$$\frac{d}{dt}K_{11}(t) = -2\left(\frac{I}{CV_T} + \frac{y_{bs}(t)}{CV_T}\right)K_{11}(t) - 2\frac{y_{as}(t)}{CV_T}K_{12}(t) + \frac{y_{as}(t)^2 I_n}{(CV_T)^2}$$

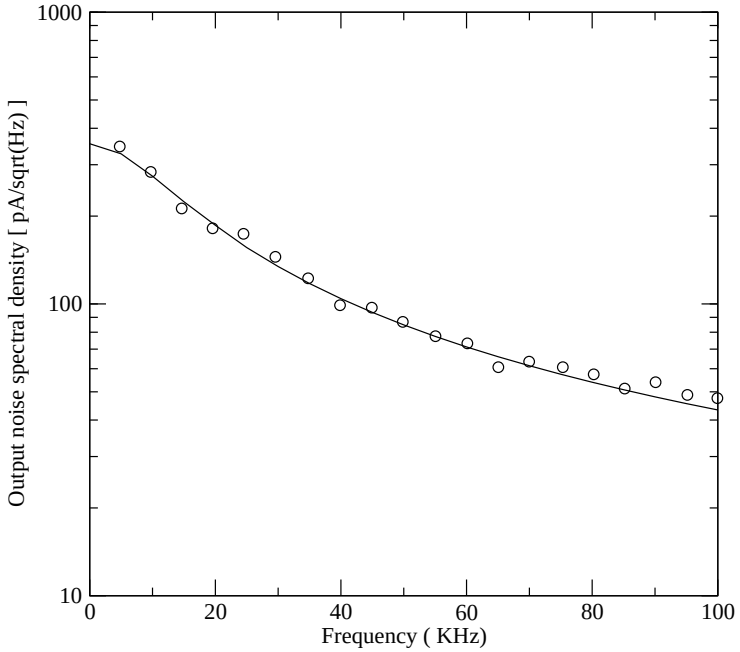

Fig. 12. Output spectral density of a class A circuit. The circles indicate published experimental data[18].

$$\frac{d}{dt}K_{12}(t) = -\frac{y_{bs}(t)}{CV_T}K_{11}(t) - \left(\frac{2I}{CV_T} + \frac{y_{as}(t)+y_{bs}(t)}{CV_T}\right)K_{12}(t) - \frac{y_{as}(t)}{CV_T}K_{22}(t)$$

$$\frac{d}{dt}K_{22}(t) = -2\left(\frac{I}{CV_T} + \frac{y_{as}(t)}{CV_T}\right)K_{22}(t) - 2\frac{y_{bs}(t)}{CV_T}K_{12}(t) \tag{35}$$

In the set of equations (35), I_n is the PSD of the input noise source and $y_{as}(t)$ and $y_{bs}(t)$ are the steady state output currents. Since the output is a differential in nature, the equations for the noise spectrum can be derived as

$$\frac{dK_1'}{dt} = -\left(\frac{I}{CV_T} + \frac{y_{bs}(t)}{CV_T}\right)K_1'(t) - \frac{y_{as}(t)}{CV_T}K_2'(t) + e^{j\omega t}(K_{11}(t) - K_{12}(t))$$

$$\frac{dK_2'}{dt} = -\left(\frac{I}{CV_T} + \frac{y_{as}(t)}{CV_T}\right)K_2'(t) - 2\frac{y_{bs}(t)}{CV_T}K_1'(t) + e^{j\omega t}(K_{12}(t) - K_{22}(t))$$

$$\frac{dK''}{dt} = 2[Re(K_1'(t))\cos(\omega t) + Im(K_1'(t))\sin(\omega t)] - 2[Re(K_2'(t))\cos(\omega t) + Im(K_2'(t))\sin(\omega t)] \tag{36}$$

Figure 13 shows that a good match is obtained between the simulated and published data. Table I shows the output SNR for various input levels. As expected, it is almost constant over the entire input range. It is about 3dB lower than published data [18]. This could be due to average output

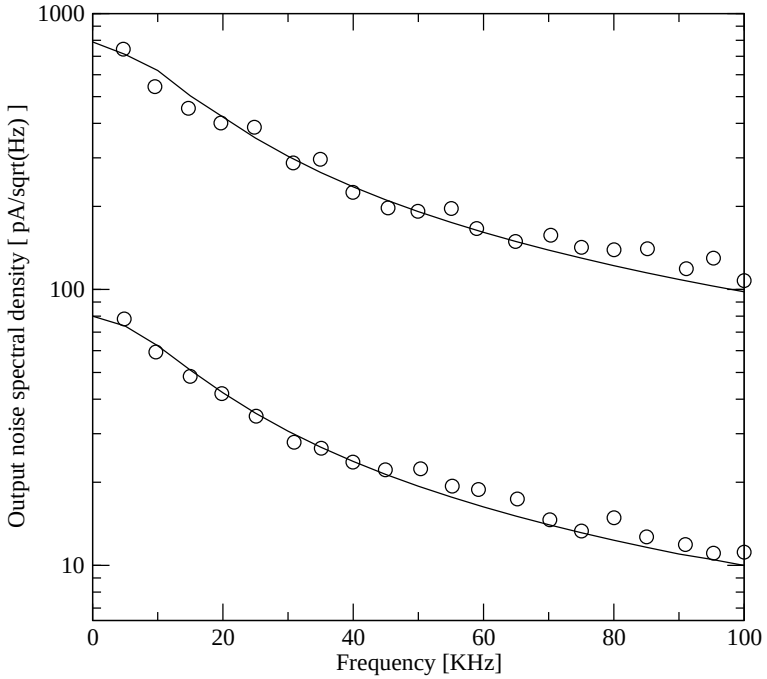

Fig. 13. Output power spectral density for a class B log domain filter. The circles indicate experimental data[18]. The two sets of curves are obtained for 10μA and 100μA peak input.

variance being used directly for SNR computations instead of integrating the output spectral density over a finite frequency range.

Peak input current(μA)	SNR (dB)
5	52.08
10	52.12
20	52.17
50	52.23
100	52.27
150	52.29
200	52.3

TABLE I

OUTPUT SNR FOR DIFFERENT VALUES OF THE INPUTS

Mulder et al [17] have obtained semi-analytical expressions for the noise spectral density and

output SNR of the Seevnick low pass filter including device noise. In this case, the noise sources are cyclostationary and there is signal-noise intermodulation. They have used averaged values of signals to compute noise intensity. In order to compare with published results, only shot noise due to the collector current has been considered in the simulations. Noise sources are assumed to be cyclostationary. The translinear principle gives the following set of equations:

$$(u_a + n(u_a))(I_o + n(I_o)) = (I + \frac{CV_T}{y_a}\frac{dy_a}{dt} + y_b + n(y_{bs}) + n(z_a))(y_a + n(y_{as}))$$

$$(u_b + n(u_b))(I_o + n(I_o)) = (I + \frac{CV_T}{y_b}\frac{dy_b}{dt} + y_a + n(y_{as}) + n(z_b))(y_b + n(y_{bs})) \tag{37}$$

where

$$n(x) = \sqrt{qx(t)}\xi_t$$

In the set of equations (37),

$$y_a = y_{as}(t) + y_{an}(t)$$

$$y_b = y_{bs}(t) + y_{bn}(t)$$

and ξ_t is a stationary white noise source with unity double sided power spectral density. The noise that is created in the output transistor due to sampled noise on capacitor ($y_{an}(t)$ and y_{bn}(t)) is seperated from the shot noise of the output transistor ($n(y_{as})$ and $n(y_{bs})$). The shot noise due to the output transistor will essentially add to the noise that is obtained by solving the above equations. u_a and u_b are the inputs and are assumed to be the output of a current splitter. The circuit operates in the class AB mode, with u_a and u_b given by:

$$u_{a,b} = \frac{1}{2}\left(\sqrt{4u_{dc}^2 + u_{in}^2} \pm u_{in}\right) \tag{38}$$

where

$$u_{in} = mI_o \sin(\omega t)$$

Including only first order noise terms, the stochastic differential equations for noise can be written as:

$$dy_{an}(t) = -\left(\frac{I_o}{CV_T} + \frac{y_{bs}(t)}{CV_T}\right) y_{an}(t)dt - \frac{y_{bs}(t)}{CV_T} y_{bn}(t)dt + \frac{\sqrt{q}}{CV_T}\mathbf{B}_1(t)d\mathbf{W}_1(t)$$

$$dy_{bn}(t) = -\left(\frac{I_o}{CV_T} + \frac{y_{bs}(t)}{CV_T}\right) y_{bn}(t)dt - \frac{y_{as}(t)}{CV_T} y_{an}(t)dt + \frac{\sqrt{q}}{CV_T}\mathbf{B}_2(t)d\mathbf{W}_2(t) \tag{39}$$

where

$$\mathbf{B}_1(t) = \left[I_o\sqrt{u_a(t)} \quad u_a(t)\sqrt{I_o} \quad y_{as}(t)\sqrt{z_a(t)} \quad y_{as}(t)\sqrt{y_{bs}(t)} \quad z_a(t)\sqrt{y_{as}(t)} \right]$$

$$\mathbf{B}_2(t) = \left[I_o\sqrt{u_b(t)} \quad u_b(t)\sqrt{I_o} \quad y_{bs}(t)\sqrt{z_b(t)} \quad y_{bs}(t)\sqrt{y_{as}(t)} \quad z_b(t)\sqrt{y_{bs}(t)} \right]$$

The shot noise current sources in different devices are uncorrelated, and are modulated by various signals in the circuit. However, there is a correlation between the noise currents in the two output transistors. This is due to the noise created in the output transistors by the sampled noise in the two capacitors (i.e $y_{bn}(t)$ sampled by the capacitor adds to $y_{an}(t)$ and vice-versa). Figure 14 shows a comparison of the SNR obtained and values published by Mulder et al [17]. For large m values, the results match very well. For low m values, results match to within $2dB$. This is possibly because Mulder *et al.* use time averaged noise sources, whereas cyclostationary sources are used in our simulations. The output noise spectral density is shown in Figure 15.

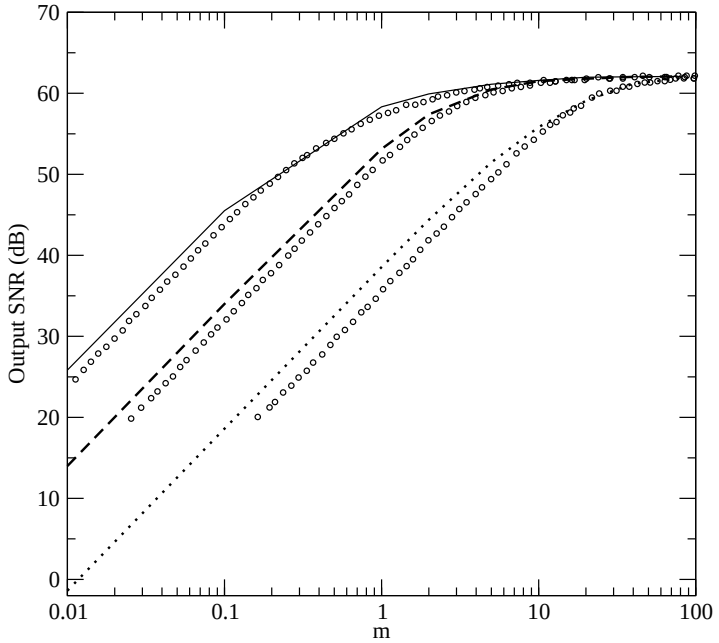

Fig. 14. Output SNR for Seevnick's class AB low pass filter. m is the scaling factor for the input signal.Circles indicate data published in [17]

The values of the currents and capacitors are $u_{dc} = 0.1\mu A$, $I_o = 1\mu A$, $m = 10$ and $C = 10pF$. For these values, the bandwidth of the low pass filter is about $612kHz$.

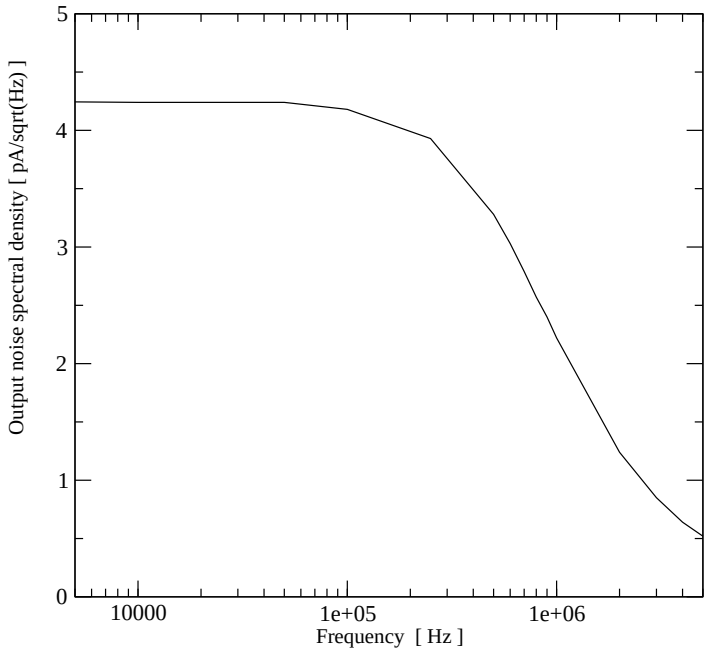

Fig. 15. Output noise spectral density for a class AB low pass filter due to shot noise in the bipolar junction transistors.

C. Phase noise in oscillators

In both SC and externally linear circuits, the covariance matrix is periodic. In oscillators, however, the envelop of the variance and cross-correlations increase with time. But the output spectrum itself is a stationary Lorentzian spectrum about each harmonic [29]. In order to understand this system better, a linear model of a ring oscillator, without any amplitude control was first considered. This is shown in Figure 16.

Using the method proposed in this paper, it is possible to get analytical expressions for the output spectrum (since the state matrix is constant). The oscillator is a 3-stage ring oscillator

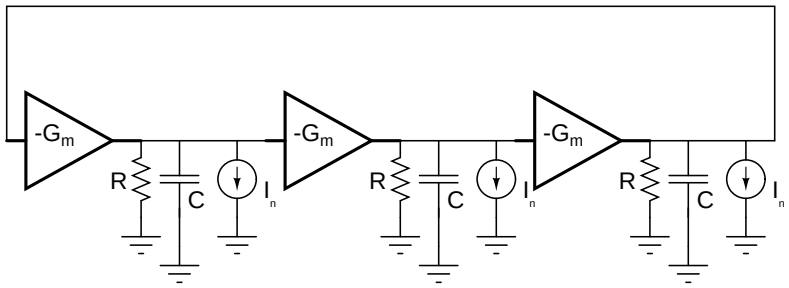

Fig. 16. Linear model of a ring oscillator

that oscillates when its loop gain becomes equal to one. This occurs for $G_m R = 2$ and $\omega_o = \frac{\sqrt{3}}{RC}$. The eigenvalues of the state matrix are $\pm\frac{j\sqrt{3}}{RC}$ and $\frac{-3}{RC}$. This implies that the eigenvalues that determine the noise covariance are $\pm\frac{2j\sqrt{3}}{RC}$, $\frac{-6}{RC}$, 0 and $\pm\frac{-3\pm j\sqrt{3}}{RC}$ i.e. besides exponentially decaying solutions, it has oscillatory solutions at twice the frequency and a solution that increases linearly with time. Using the eigenvalues and eigenvectors, the solutions for the variance at the three nodes and the cross-correlations can be obtained. Zero initial conditions are assumed. Only thermal noise due to resistors is considered.

It turns out that all three nodes have the same variance. This is as expected [29]. The three cross-correlations are also equal to each other. The variance (V) and the cross-correlations (K) are given by:

$$V = \frac{R^2}{36\sqrt{3}}\omega_o I_n (1 - e^{\frac{-6t}{RC}}) + \left[\frac{R^2}{9}\omega_o^2 I_n\right] t$$
$$K = \frac{R^2}{36\sqrt{3}}\omega_o I_n (1 - e^{\frac{-6t}{RC}}) - \left[\frac{R^2}{18}\omega_o^2 I_n\right] t \tag{40}$$

where $I_n = \frac{4KT}{R}$. The variance increases linearly with time and the cross-correlations decrease linearly with time at half the rate at which the variance increases.

An analytical expression for the power spectral density can be obtained using the eigenvalues and eigenvectors of the state matrix. Ignoring exponentially decaying terms, the power spectral density is obtained as:

$$PSD = \frac{6A}{RC}\frac{1}{\omega^2 + 3\omega_o^2} + 2B\frac{(\omega^2 + \omega_o^2)}{\left(\omega^2 - {\omega_o}^2\right)^2} - \lim_{t\to\infty}\left\{2B\frac{(\omega^2 + {\omega_o}^2)}{\left(\omega^2 - {\omega_o}^2\right)^2}\frac{sin((\omega - \omega_o)t))}{(\omega - \omega_o)t}\right\} \tag{41}$$

where

$$A = \frac{R^2}{36\sqrt{3}}\omega_o I_n, \qquad B = \frac{R^2}{9}\omega_o^2 I_n$$

In the limit, the third term tends to zero. For frequencies close to ω_o, the power spectral density can be approximated to:

$$PSD = \frac{B}{\Delta\omega^2} \tag{42}$$

Here $\Delta\omega$ represents the offset from the oscillation frequency. Equation (42) is the same as the expression obtained earlier by Razavi [21] for additive noise in a linear oscillator, close to the frequency of oscillation. This is expected, since the oscillator is modeled as a linear time-invariant (though unstable) system. In fact, if the first term in the expression for the PSD is set

to zero and the singularity is shifted from ω_o to zero, we get the power spectral density of an ideal integrator with white noise input.

Equation (41) also gives some insight into the convergence behaviour of the power spectral density. It is governed by the rate at which the third term in the expression for the power spectral density approaches zero. Clearly, as the frequency of measurement approaches the frequency of oscillation, it takes much longer for the power spectral density to approach a steady state value.

A three stage ring oscillator shown in Figure 17 was then simulated. Once again, only the thermal noise due to the resistors was considered. The state equations used for this oscillator

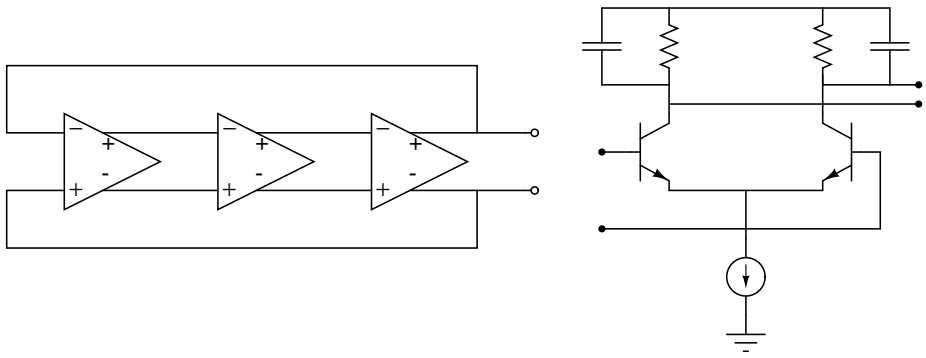

Fig. 17. Three stage ring oscillator - block diagram and the delay cell.

were assumed to be the following.:

$$\begin{aligned}
\frac{dV_1}{dt} &= -\frac{V_1}{2RC} - \frac{I_b}{2C} tanh\left(\frac{V_3}{2\eta V_T}\right) \\
\frac{dV_2}{dt} &= -\frac{V_2}{2RC} - \frac{I_b}{2C} tanh\left(\frac{V_1}{2\eta V_T}\right) \\
\frac{dV_3}{dt} &= -\frac{V_3}{2RC} - \frac{I_b}{2C} tanh\left(\frac{V_2}{2\eta V_T}\right)
\end{aligned} \tag{43}$$

The values used for the simulation are $R = 2k\Omega$, $C = 1pF$, $I_b = 10^{-4}A$, $V_T = \frac{KT}{q}$ and $\eta = 1$. For these values, the frequency of oscillation is $70.4MHz$. The perturbed equations were used to find the noise variance and the cross-correlations. As expected, it is an oscillatory waveform with a linearly increasing envelop [29].

The power spectral density was simulated using the algorithm proposed in this paper. Figure 18 shows the single sideband phase noise spectrum in dBc/Hz. The results are compared

with the data obtained using the analytical formula derived by Demir *et* al [29]. They show that the single sideband spectrum can be written as:

$$\mathcal{L}(f_m) = 10log_{10}\left(\frac{f_o^2 c}{\pi^2 f_o^4 c^2 + f_m^2}\right), \quad 0 \leq f_m << f_o \tag{44}$$

where f_m is the frequency offset from the oscillation frequency f_o. The parameter c is defined as:

$$c = B/S^2$$

where B is the slope of the variance curve and S is the derivative of the large signal solution at the zero-crossings. The data in the figure was computed using the values of B, c and f_o obtained from the variance and large signal simulations. The results match to within $1dBc/Hz$.

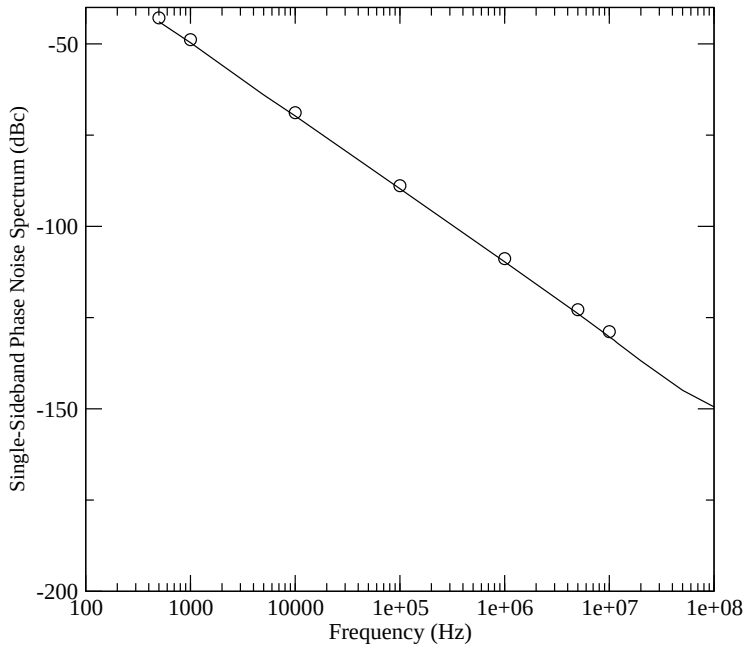

Fig. 18. Single-Sideband phase noise spectrum of the oscillator. The circles indicate data obtained using an analytical formula derived by Demir *et* al[29].

Clearly, this method can be used to get the noise spectrum of the oscillator. Both stationary and cyclostationary noise sources can be used. Unlike some previous methods [28], [31], we do not need to do an orthogonal decomposition for amplitude and phase noise. Both are taken care of simultaneously. However, it has some limitations. As the frequency of "measurement" approaches the oscillator frequency, the time required for convergence increases as indicated by equation (41). In this particular case, computation of the spectrum within $500Hz$ of the

frequency of oscillation proved to be difficult. The convergence behaviour is similar to that of the linear oscillator and it takes a very long time to reach steady state. Also, for these frequencies, the perturbation model can no longer be used and non-linearities have to be taken into account.

VI. CONCLUSIONS

A new time-domain technique to get the average power spectral density of noise is proposed. The thrust of this study was to look at the possiblity of using the algorithm in a variety of circuits. To validate the method, it has been used to simulate the noise spectral density in switched capacitor circuits, externally linear circuits and in oscillators. The results match well with published experimental/analytic data. Simple macromodels were used. However, to get a more accurate noise response, better device models and $1/f$ noise sources need to be included. Also, more efficient numerical methods can be used to speed up the code. This is currently being studied.

Since it is based on stochastic differential equations, it has all the advantages and disadvantages of the method. Its principal advantage is that it can be used for any circuit that can be analyzed using the transient analysis routine of the circuit simulator, even those in which the noise is non-stationary. Both the variance and the PSD of noise can be obtained. It can be also very easily integrated into a standard circuit simulator. Since the spectrum is obtained based on time-varying cross-correlations, the relative contribution of various portions of the circuit to the output noise spectrum can be obtained. However, computationally it is restricted to relatively small blocks, mainly because for an N node circuit, $\frac{N(N+1)}{2}$ equations have to be solved to get the time-varying covariance matrix. Also, $1/f$ can only be included if appropriate filtering networks are used [32], [35]. However, it is not clear how efficient this is, since it adds to the equations already present. It is clear that the method can be used very effectively if the noise simulation is done in a hierarchical fashion, building good macromodels at each stage.

ACKNOWLEDGEMENT

The author would like to thank Dr.M.Ramakrishna for useful technical discussions, help with the figures and careful reading of the manuscript. This work was possible only because of all the people contributing to the open source software.

REFERENCES

[1] R.Rohrer, L.Nagel, R.Meyer, and L.Weber, "Computationally efficient electronic-circuit noise calculations," *IEEE J.Solid-State Circuits*, vol. SC-6, pp. 204–213, 1971.

[2] S.O.Rice, "Response of periodically varying systems to noise-application to switched RC circuits," *Bell Syst. Tech. J.*, vol. 49, pp. 2221–2247, Nov. 1970.

[3] T.Strom and S.Signell, "Analysis of periodically switched linear circuits," *IEEE Trans. Circuits Syst.*, vol. CAS-24, pp. 531–541, Oct. 1977.

[4] J.H.Fisher, "Noise sources and calculation techniques for switched capacitor filters," *IEEE J. Solid State Circuits*, vol. SC-17, pp. 742–752, Aug 1982.

[5] F. F.Maloberti and V.Svelto, "Noise and gain in a SC integrator with real operational amplifier," *Alta Frequenza*, vol. L, no. 1, pp. 4–11, 1981.

[6] J.Goette and C.Gobet, "Exact noise analysis of SC circuits and an approximate computer implementation," *IEEE Trans. Circuits and Syst.*, vol. 3, pp. 508–521, April 1989.

[7] C.Gobet and A.Knob, "Noise analysis of switched capacitor networks," *IEEE Trans. Circuits and Syst.*, vol. CAS-30, pp. 37–43, Jan 1983.

[8] L.Toth, I.Yusim, and K.Suyama, "Noise analysis of ideal switched-capacitor networks," *IEEE Trans. Circuits and Syst.-I*, vol. 46, pp. 349–363, March 1999.

[9] J.Vandewalle, H. D. Man, and J.Rabaey, "The adjoint switched capacitor network and its application to frequency,noise and sensitivity analysis," *Int. J.Circuit Theory Appl*, vol. 9, pp. 77–88, 1981.

[10] Z.Q.Shang and J.I.Sewell, "Efficient noise analysis methods for large nonideal SC and SI circuits," in *Proc.IEEE ISCAS*, (Piscataway, NJ), pp. 565–568, 1994.

[11] F.Yuan and A.Opal, "Noise and sensitivity analysis of periodically switched linear circuits in frequency domain," *IEEE Trans. Circuits and Syst.-I*, vol. 47, pp. 986–998, July 2000.

[12] F.Yuan and A.Opal, "Adjoint network of periodically switched linear circuits with applications to noise analysis," *IEEE Trans. Circuits and Syst.-I*, vol. 48, pp. 139–151, Feb. 2001.

[13] Y.Dong and A.Opal, "Time-domain thermal noise simulation of switched-capacitor circuits and delta-sigma modulators," *IEEE Trans. Computer Aided Design*, vol. 19, pp. 473–481, April 2000.

[14] M.Okumura, H.Tanimoto, T.Itakura, and T.Sugawara, "Numerical noise analysis for nonlinear ciruits with a periodic large signal excitation including cyclostationary noise sources," *IEEE Trans. Circuits and Syst.-I*, vol. 40, pp. 581–590, Sept. 1993.

[15] J.Roychowdhury, D.Long, and P.Feldmann, "Cyclostationary noise analysis of large RF circuits with multitone excitations," *IEEE J.Solid-State Circuits*, vol. 33, pp. 324–336, March 1998.

[16] M.H.L.Kouwenhowen, J.Mulder, W.A.Serdjin, and A. Roermund, "Noise analysis of dynamically nonlinear translinear circuits," *Electron. Letters*, vol. 34, pp. 705–706, April 1998.

[17] J.Mulder, M.H.L.Kouwenhowen, W.A.Serdjin, A. der Woerd, and A. Roermund, "Nonlinear analysis of noise in static and dynamic translinear circuits," *IEEE Trans. Circuits Syst. II*, vol. 46, pp. 266–277, March 1999.

[18] L.Toth, Y.P.Tsividis, and N.Krishnapura, "On the analysis of noise and interference in instantaneously companding signal processors," *IEEE Trans. Circuits and Syst.-II*, vol. 45, pp. 1242–1249, Sept. 1998.

[19] L.Toth, G.Efthivoulidis, and Y.P.Tsividis, "Noise analysis of externally linear systems," *IEEE Trans. Circuits and Syst.-II*, vol. 47, pp. 1365–1377, Dec. 2000.

[20] D.B.Leeson, "A simple model for the feedback oscillator noise spectrum," *Proc. IEEE*, vol. 54, pp. 329–330, Feb. 1966.

[21] B.Razavi, "A study of phase noise in CMOS oscillators," *IEEE J. Solid-State Ckts.*, vol. 31, pp. 331–343, March 1996.

[22] J.McNeill, "Jitter in ring oscillators," in *Proc. ISCAS*, pp. 27–30, June 1994.

[23] T.Weigandt, B.Kim, and P.R.Gray, "Analysis of timing jitter in cmos ring oscillators," in *Proc. ISCAS*, pp. 201–204, June 1994.

[24] A.A.Abidi and R.Meyer, "Noise in relaxation oscillators," *IEEE J.Solid-State Circuits*, vol. SC-18, pp. 794–802, Dec. 1983.

[25] K.Kurokawa, "Noise in synchronised oscillators," *IEEE trans. microwave theory and tech.*, vol. MTT-16, pp. 234–240, April 1968.

[26] M.Okumura and H.Tanimoto, "A time-domain method for numerical noise analysis of oscillators," in *Proc. DAC*.

[27] B. D. anf G.Gielen, "Accurate simulation of phase noise in oscillators," in *European Solid-State Circuits Conf*, pp. 204–208, 1997.

[28] A.Hajimiri and T.H.Lee, "A general theory of phase noise in oscillators," *IEEE J.Solid-State Circuits*, vol. 33, pp. 179–194, Feb. 1998.

[29] A.Demir, A.Mehrotra, and J.Roychowdhury, "Phase noise in oscillators: A unifying theory and numerical methods for characterization," *IEEE Trans. Circuits and Syst.-I*, vol. 47, pp. 655–674, May 2000.

[30] M.Lax, "Classical noise v. noise in self-sustained oscillators," *Physical Review*, vol. 160, pp. 290–307, Aug. 1967.

[31] F.Kaertner, "Analysis of white and $f^{-\alpha}$ noise in oscillators," *International Journal of Circuit Theory and Applications*, vol. 18, pp. 485–519, 1990.

[32] A.Demir, E.W.Y.Liu, and A.L.Sangiovanni-Vincentelli, "Time-domain non-Monte Carlo noise simulation for nonlinear dynamic circuits with arbitrary excitations," *IEEE Trans. Computer Aided Design*, vol. 15, pp. 493–505, May 1996.

[33] A.Mehrotra, "Noise analysis of phase locked loops," *IEEE Trans. Circuits and Syst.-I*, vol. 49, pp. 1309–1316, Sept. 2002.

[34] Y.Degerli, F.Lavernhe, P.Magnan, and J.Farre, "Non-stationary noise responses of some fully differential on-chip readout circuits suitable for CMOS image sensors," *IEEE Trans. Ckts. Syst. II*, vol. 46, pp. 1461–1474, Dec. 1999.

[35] W.A.Gardner, *Introduction to Random Processes:with applications to signals and systems*. New York: McGraw-Hill, 1989.

[36] M.J.Buckingham, *Noise in Electronic Devices and Systems*. Ellis Horwood Limited, 1983.

[37] D.G.Lampard, "Generalization of the weiner-khintchine theorem to nonstationary processes," *J.Appl. Physics*, vol. 25, no. 6, pp. 802–803, 1952.

[38] A.Demir, *Analysis and Simulation of Noise in Nonlinear Electronic circuits and systems*. PhD thesis, University of California, Berkeley, 1997.

[39] C.W.Gardiner, *Handbook of Stochastic methods for Physics, Chemistry and the Natural Sciences*. New York: Springer-Verlag, 1983.

[40] B. Oksendal, *Stochastic Differential Equations*. Springer-Verlag, 5 ed., 1998.

[41] S. Shreve, "Lectures on stochastic calculus and finanace." www-2.cs.cmu.edu/ shreve/shreve.pdf.

[42] V.Vasudevan and M.Ramakrishna, "Computation of noise spectral density in switched capacitor circuits using the mixed-frequency-time technique." Submitted to the Design Automation Conference.

[43] S.-C. Fang, Y.Tsividis, and O.Wing, "Time- and frequency-domain analysis of linear switched-capacitor networks using state charge variables," *IEEE Trans. Computer Aided Design*, pp. 651–661, Oct 1985.

[44] L.Toth and K.Suyama, "Exact noise analysis of ideal swiched-capacitor networks," in *Proc. IEEE ISCAS*, pp. 1585–1588, May 1996.

[45] E.Seevnick, "Companding current-mode integrator: A new circuit principle for continuous-time monolithic filters," *Electron. Letters*, vol. 26, pp. 2046–2047, Nov. 1990.

Manuscript Received:

Affiliation of Author: Department of Electrical Engineering, Indian Institute of Technology-Madras

LIST OF FIGURES